BERKELEY LAB

EGS Collab Experiment 2

Passive seismic monitoring system

Report no: LBNL-2001514
LBNL EESA
March 2023

AUTHOR (Last, First):
Hopp, Chet
DATE:
3-24-2023
TITLE:
EGS Collab Experiment 2: Passive seismic monitoring system

Contents

1 Terminology

- **SURF**: Sanford Underground Research Facility. The old Homestake gold mine in Lead, SD, USA where the EGS Collab experiment has taken place.
- **OD**: Outer diameter
- **ERT**: Electrical Resistivity Tomography
- **CASSM**: Continuous Active Source Seismic Monitoring. A network of piezoelectric sources and seismic receivers for cross-well seismic tomography.
- **LBNL or LBL**: Lawrence Berkeley National Lab (Berkeley, CA)
- **SNL**: Sandia National Lab (Albuquerque, NM)
- **PNNL**: Pacific Northwest National Lab (Richland, WA)

2 Introduction

The EGS Collab Experiment #2 took place from approximately February–September 2022 at the Sanford Underground Research Facility in Lead, SD. The project was the continuation of a years-long experiment aiming to validate models of enhanced geothermal systems through a series of high-pressure injections into rock between 1200 and 1500 meters below the surface. These injection experiments were extensively monitored by a number of systems including seismic waveform recording, pressure and temperature probes, active source seismic tomography, electrical resistivity tomography, and a full suite of distributed fiber optic interrogators.

This report details the passive seismic monitoring system that monitored, in real time, the timing and location of small earthquakes in the testbed resulting from the injection of fluid and fracturing of the rock. This monitoring system consisted of accelerometers and hydrophones placed in various boreholes surrounding the injection zones and operated continuously throughout the experiment.

3 Installation

The passive seismic monitoring system for EGS Collab Experiment 2 consisted of two types of seismic sensors: piezoelectric accelerometers and hydrophones. These sensors were recorded by two different recording systems each targeting a different application. One recording system recorded 64-channels of data continuously for the purpose of monitoring for seismicity that was induced and/or triggered by the injection operations. These data were processed in real-time in an attempt to monitor seismicity to inform decision-making during the experiment. The other recording system recorded the same sensors only at a lower sampling rate and in triggered mode. This system was a part of an active-source monitoring system called CASSM (Continuous Active-Source Seismic Monitoring) that uses waves emitted from custom-built piezoelectric sources installed in the boreholes to estimate various properties of the rock volume with time. While the sensors are common across both systems, this report focuses on the continuous, high-frequency recording system.

3.1 Sensors

The piezoelectric accelerometers were manufactured by MMF of Germany. They are model KS943B100 triaxial sensors that conform to the IEPE (Integrated Electronics Piezo Electric) standard. They have a sensitivity of 100 mV/g (the sensors installed on the 4850 level for EGS Collab Experiment 1 had a sensitivity of 1 V/g) and a linear frequency response range of 0.5 Hz to 22 kHz within 3 dB. The full specsheet can be found here. Each of the 16 MMF accelerometers was packaged into a stainless steel housing at the Geosciences Measurement Facility (GMF) at LBNL (Figure 6A and B). Calibration certificates for three of these accelerometers were purchased and are included in the GDR submission for the continuous waveform data. For analyses requiring correction of the data to real units (i.e. sensor frequency response removal) the user is directed to these certificates that can be used to construct sensor response files. While some minor discrepancies exist between sensors, we feel it is reasonable to treat all sensors as having a response curve equivalent to the average of these three calibration curves.

A string of 24 hydrophones was installed in one of the open boreholes, TS (water-coupled; not grouted). This string consisted of HTI-96-MIN/V 5/8 sensors manufactured by High Tech, Inc. The hydrophones have a flat frequency response from 2 Hz to 2 kHz. Due to a misunderstanding in the ordering process, a 2 kHz hardware lowpass-filter was installed. This means that much of the anticipated frequency content of the seismicity for this experiment (into the 10s of kHz) was not recorded on these instruments. The array had an inter-sensor spacing of 2.5 m.

Finally, 20 active seismic sources were installed. These sources are cylindrical piezoelectric crystals manufactured at the Geosciences Measurement Facility at LBNL. Sources are fired by applying a voltage to the piezoelectric ceramic and the signal is recorded across the

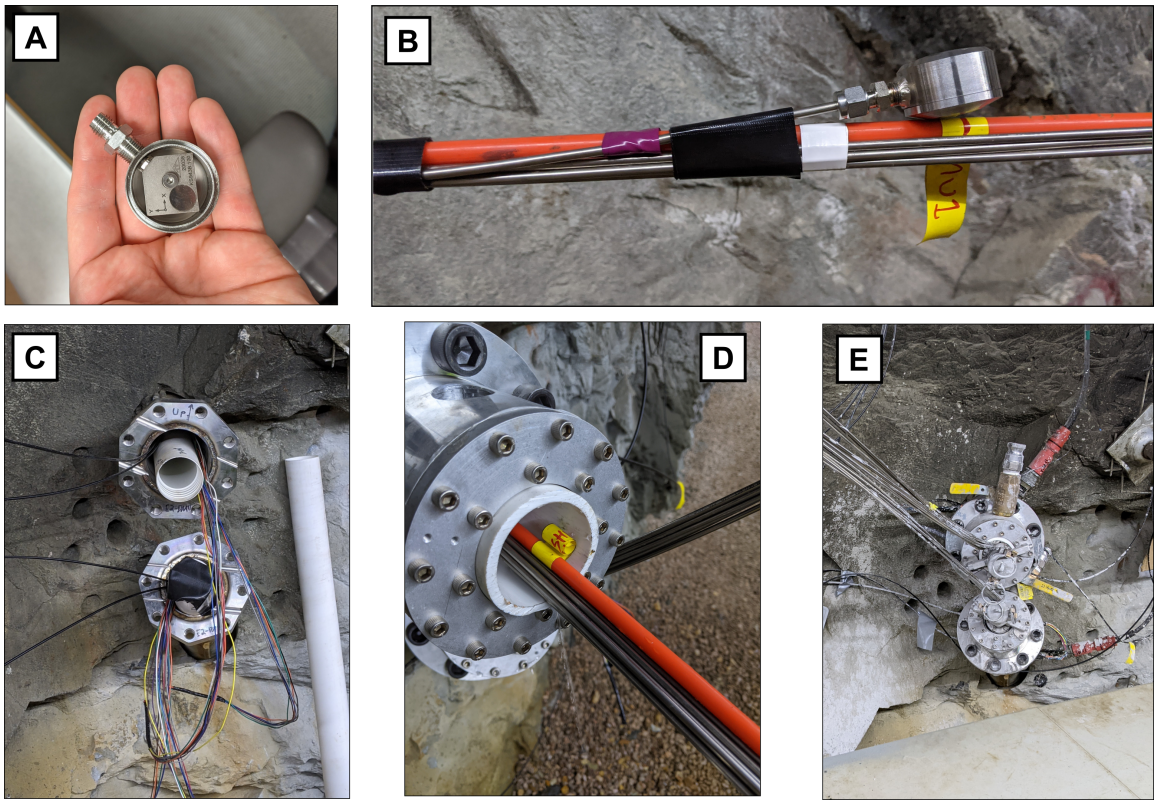

Figure 1: Pictures of the various stages of accelerometer fabrication and installation. A) A single triaxial accelerometer inside an open steel housing B) Completed housing attached to TEC and taped to a conveyance rod (orange fiberglass). C) Schedule 40 PVC shrouds protruding from the wellheads. These were necessary to isolate the ERT electrodes from all of the metal involved in the wiring and housings for the seismic sensors. D) The wellheads were sealed off using a custom machined cap from SNL that left the inside of the shroud open to lower the seismic sensor package E) Final state of the fully grouted boreholes DMU and DML with all sensor cables fed through the wellcaps.

array of sensors described above. This system is known as Continuous Active Source Seismic Monitoring or CASSM [2].

To protect the cables as they ran up the grouted boreholes, stainless steel tubing encapsulated cable (TEC) was used. This choice was made mostly to avoid fluid infiltrating the CASSM sources and accelerometers, which damaged a number of sensors in Experiment #1 on the 4850 level of the mine.

3.2 Borehole array design

Each of the monitoring array boreholes needed to fit many different sets of sensing equipment, each with unique requirements. This equipment included not only the seismic sensors and their cables, but also a steel encased fiber optics package and also a number of electrodes for the electrical resistivity tomography (ERT) system. One major consideration was that any metal in the borehole would severely interfere with the ERT system and would therefore need to be electrically isolated. This was done by placing all of the seismic instrumentation inside a 2.5-inch schedule 40 PVC "shroud". The ERT electrodes were strapped to the outside of the shroud along with the fiber optic package (which was steel encapsulated but coated in a non-conductive material). The one non-grouted monitoring borehole, TS, was designed in a similar way, with the exception being that it contained no steel cables for the CASSM sources or the hydrophone string (they were plastic coated instead). Cross sections for both grouted and non-grouted boreholes are shown in Appendix 6.4.

3.3 Array layout

Figure 2 shows the geometry of the seismic array with grouted boreholes shown in black, open boreholes shown in blue, and seismic sensors shown as red inverted triangles.

Each of the grouted boreholes contained four CASSM sources and four three-component accelerometers. The spacing and location of these instruments were chosen to maximize the ability of the accelerometers to constrain the location and mechanism of detected seismicity as well as to maximize the raypath coverage of the CASSM system. In borehole TS, four CASSM sources were installed alongside the 24-channel hydrophone array. The locations for each sensor are given in Table 3 within the Homestake Mine Coordinate system. This is a cartesian system used for most data coming out of the mine. Units are given in feet.

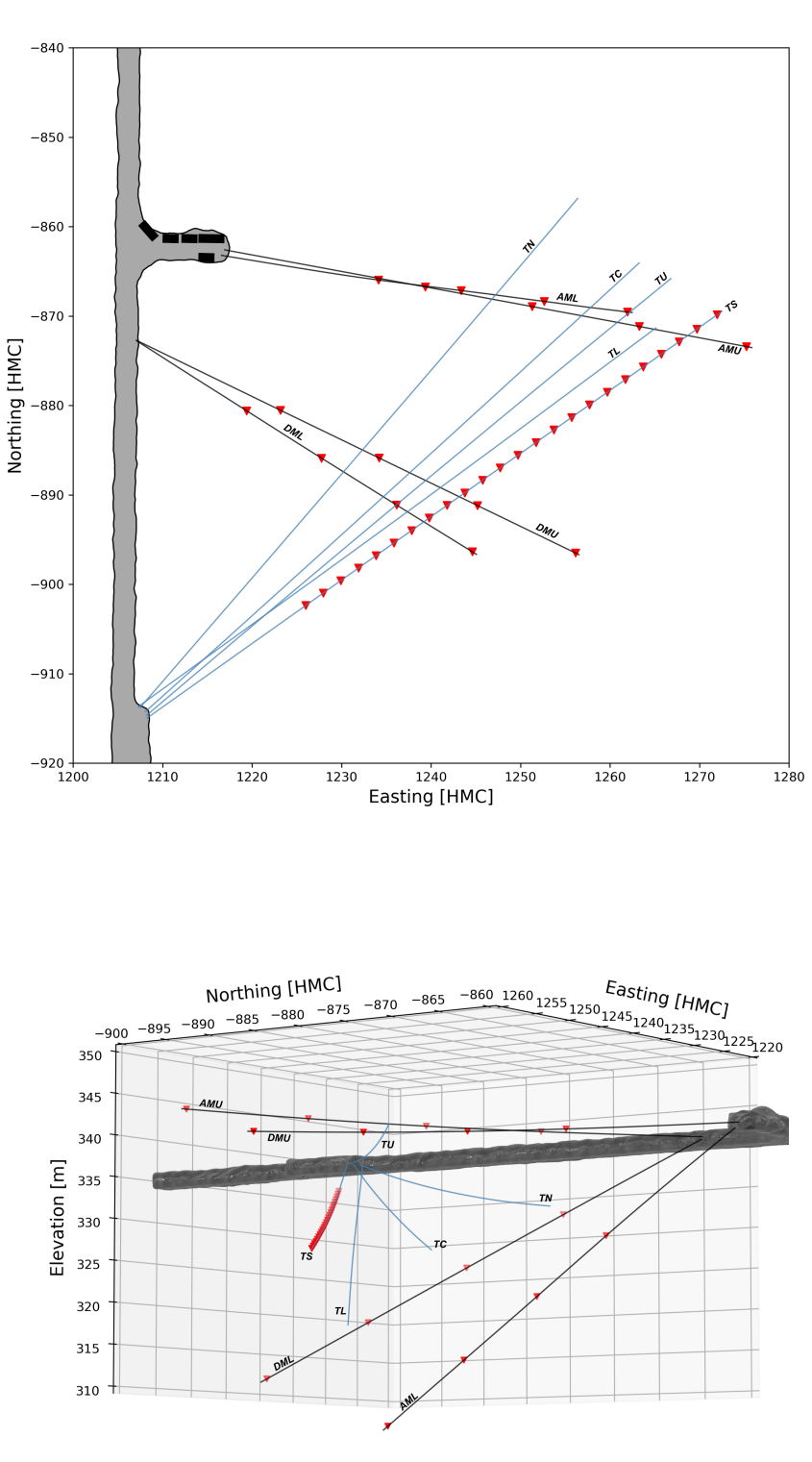

Figure 2: Overview of the EGS Collab Experiment 2 testbed on the 4100 level of SURF. The boreholes are labeled by name and the locations of the seismic sensors are indicated with red triangles. The fiber loop is installed in the four grouted boreholes (AMU, AML, DMU, and DML) shown in black. A string of hydrophones is installed in non-grouted borehole TS.

3.4 Recording systems

Two recording systems were used to digitize the data coming from the accelerometers and hydrophones; one in continous recording mode and the other in triggered recording mode. The continuous data recorder was a 64-channel VIBbox-64 manufactured by Data Translation. This system recorded each channel of the three-component accelerometers and half of the hydrophone channels at a sampling rate of 100 kHz. The triggered system was an interconnected series of Geometrics Geode seismographs, which were triggered to record based on the shot times of the CASSM sources. This system recorded each available channel from all sensors. The full CASSM system is explained in greater detail in a separate submission to the Geothermal Data Repository.

4 Data

This section describes the raw data and data products produced by the Data Translation VIBbox continuous recorder. The triggered recordings from the CASSM system are detailed in a separate report within the relevant GDR submission for the CASSM dataset.

4.1 Raw data

The data from the VIBbox-64 were saved as 32-bit binary files, each containing 32 seconds of data from 64 channels. Each file consists of header values (the first 148 bytes) followed by the data itself, which are stored as 32-bit unsigned integers. The gain of the system was set to x100, corresponding to ±0.1 V input.

We use the SEED convention in naming each channel coming in from the sensors. This consists of four fields: network, station, location, and channel, and is written like `NET.STA.LOC.CHAN`. We named the network CB (CollaB). The stations are named for the borehole that the sensor is installed in (up to 5 characters) and its relative depth in the borehole (1 to 4 for increasing depth). For example, the Z channel for station AMU1 would be written as `CB.AMU1..XNZ`. The location code is omitted as it is not useful in this case. Please refer to the SEED channel naming convention for information on channel naming. The order in which the data are stored to disk is indicated in Appendix Table 2. Note that not all of the hydrophone channels were recorded on the VIBbox because we had more than 64 channels available. Therefore we recorded only the even-numbered hydrophone channels. We also included three CASSM-specific channels in the data: CMon, CTrg, and CEnc. CTrg records the trigger signal sent to the CASSM source and CEnc encodes which source is being fired. These data were recorded to help remove active source shots from the processing of the VIBbox data, which was focused on passive-source seismicity. The final channel, CB.PPS.., is a time signal, one square wave per second from a Rubidium clock-backed PTP server installed with the rest of our monitoring equipment. The onset of the square wave corresponds to the start of a second.

Appendix 6.3 provides a Python function to read a single VIBbox binary file to an Obspy Stream object. For those unfamiliar with the Obspy Python package, it is an extremely useful tool for manipulating and processing seismic data in the Python ecosystem. Its documentation can be found here.

4.2 Realtime seismicity processing

During EGS Collab Experiment #2, we processed the VIBbox data in near realtime in order to use the location of seismic events to inform decision-making. To do this, we used a modified version of the software program DUGseis. Because we were unable to get the VIBbox to write to the HDF5-based format required by the software, many modifications

were necessary to the source code and some features (e.g. interactive phase picking and plotting) were eliminated. The final version of the code used on the 4100 level can be found in the `lbl_dev` branch of my fork of the DUGseis repository here. The realtime system worked well until early June 2022, when we filled our fast network attached storage (NAS) systems and needed to write VIBbox data to external hard drives while we sent the NAS drives back to LBL to be emptied and swapped. Writing to the external drives was too slow for the realtime system to keep pace effectively. Data following approximately June 5 were processed at LBNL after the experiment was demobilized (at the time of writing in March 2023, this effort was ongoing). The output from the system included automatic event detection, location, and magnitude estimation.

4.3 Noise sources and other data quality notes

With so much activity in the drift and so many different monitoring systems operating in the same boreholes, users are warned that the continuous VIBbox data have a number of data quality issues that are important to understand.

4.3.1 CASSM shots

The CASSM system ran nearly continuously from March 17 until September 12, 2022. The system cycled through each of the 20 sources in succession, firing 16 shots at one-second intervals, waiting a number of seconds to stack the signals, and then moving to the next source. These signals dominate the continuous seismic records and must be either removed or ignored to effectively identify any seismicity related to injection activities. As mentioned above, the CASSM signals are somewhat easy to remove once they are detected because the known source waveform is recorded in the CB.CTrg channel.

4.3.2 ERT cross-talk

Another system that was operating during the entirety of the experiment was the Electrical Resistivity Tomography (ERT) system. This system consisted of a number of electrodes, installed in the same boreholes as the seismic sensors, that both sent and received electrical signals across the testbed. As discussed in the installation section, an effort was made to electrically isolate the ERT and seismic instrumentation from each other using a schedule 40 PVC shroud. However, while this was effective in eliminating the effect of the TEC and metal sensor enclosures on the ERT system, the reverse was not true. ERT signals appear as large spikes in the continuous data, varying in shape depending on the location of the source electrode relative to the seismic sensor in question, but occurring at roughly the same time across all channels. These types of signals are difficult to remove, especially in a realtime application where speed is of the highest priority. The approach we settled on was to use matched filter detection techniques, in this case a Python pack-

age called EQcorrscan [1], to find occurrences of ERT cross-talk and remove them from the data. We manually selected ten ERT spikes for all 64-channels of data and scanned these template events through each 32-second chunk of data. Where any of the templates matched the continuous data, we removed that section of data and linearly interpolated over the gap. Finally, we overprinted the filled gap with artificial noise created by drawing from a random normal distribution scaled to the median absolute deviation of the entire 32-second trace. This technique proved capable of detecting and eliminating at least 95% of the ERT cross-talk spikes from the data.

4.3.3 Blast shots

Far less common, but important to note, were the occurrences of blasting shots conducted for the excavation of large caverns on the 4850 level. These occurred up to twice a day at recorded intervals. Because the site of the blasting is more than one kilometer from the EGS Collab site, the frequency of these waves recorded by the hydrophones and accelerometers in our boreholes is too low to adversely affect the detection of the small events of interest to us. But these blasts are visible in the data and could be made use of by other researchers with different aims. Please consult SURF directly for records of the timing and location of these blasts.

4.3.4 VIBbox hardware malfunction: 7-9-2022

At 14:03:50.412766 UTC on July 9, 2022, during the chilled water circulation test, the VIBbox interrogator suffered a hardware malfunction. The cause is unknown as of this writing, but the result was that eight channels swapped their write order in the raw data files. This was only discovered months after the experiment had been completely decommissioned, but the malfunction partly contributed to the failure of the realtime system during EGS Collab Experiment 2 (and 3). Table 1 describes which channels were affected and the channel they changed places with after the hardware issue. This issue is still under investigation the time of writing. If any user wants to analyze VIBbox data from after this malfunction, please reach out to chopp@lbl.gov to see if we've reached a resolution after this report's publication.

Original SEED ID	Original write position	New write position
CB.PPS..	64	8
CB.CEnc..	63	9
CB.CMon..	61	10
CB.Trig..	62	11
CB.TS16..XDH	8	64
CB.TS18..XDH	9	63
CB.TS20..XDH	10	61
CB.TS22..XDH	11	62

Table 1: Original and new channel ordering following the VIBbox malfunction on 7-9-2022.

4.4 Sensor calibration and frequency response information

As mentioned briefly above, we purchased calibration certificates for three of the 16 installed accelerometers. These certificates provide detailed information about the response of the sensors to excitation at known frequencies and can therefore be used to construct frequency response curves. These certificates are included in the GDR submission with the VIBbox dataset and Figure 3 shows the acceleration amplitude and phase response from these calibrations. The shake tests were only conducted up to 20 kHz, so users are cautioned against correcting for instrument response at frequencies higher than this. These results apply only to the bare accelerometers themselves and do not account for the effect of the enclosures or the grouting on the frequency response convolved into the data.

To help combat the unknowns mentioned above, we conducted a series of calibration shots along the rib of the main drift. We used an automatic, adjustable center punch tool with a known striking force of 250 N (Rennsteig model #430 231). 11 points were surveyed along the main drift rib starting north of the Site A alcove and running to south of the Site B excavation. Seven surveys were carried out during the duration of the experiment, with each survey consisting of a single sweep along all 11 shot points. At each shot point, we began with a single blow from a 5 lb sledgehammer, followed by 10 shots from the center punch. The locations of the 11 shot points are recorded in Appendix 4 and the approximate time and shot point for each hammer blow is shown in Appendix 5. Unfortunately, we were unable to trigger the Geodes in the CASSM system to record on the hammer or center punch shots as we did not have a trigger cable long enough to span the entire survey area. Analyses of these shots must therefore be conducted manually using the continuous VIBbox data.

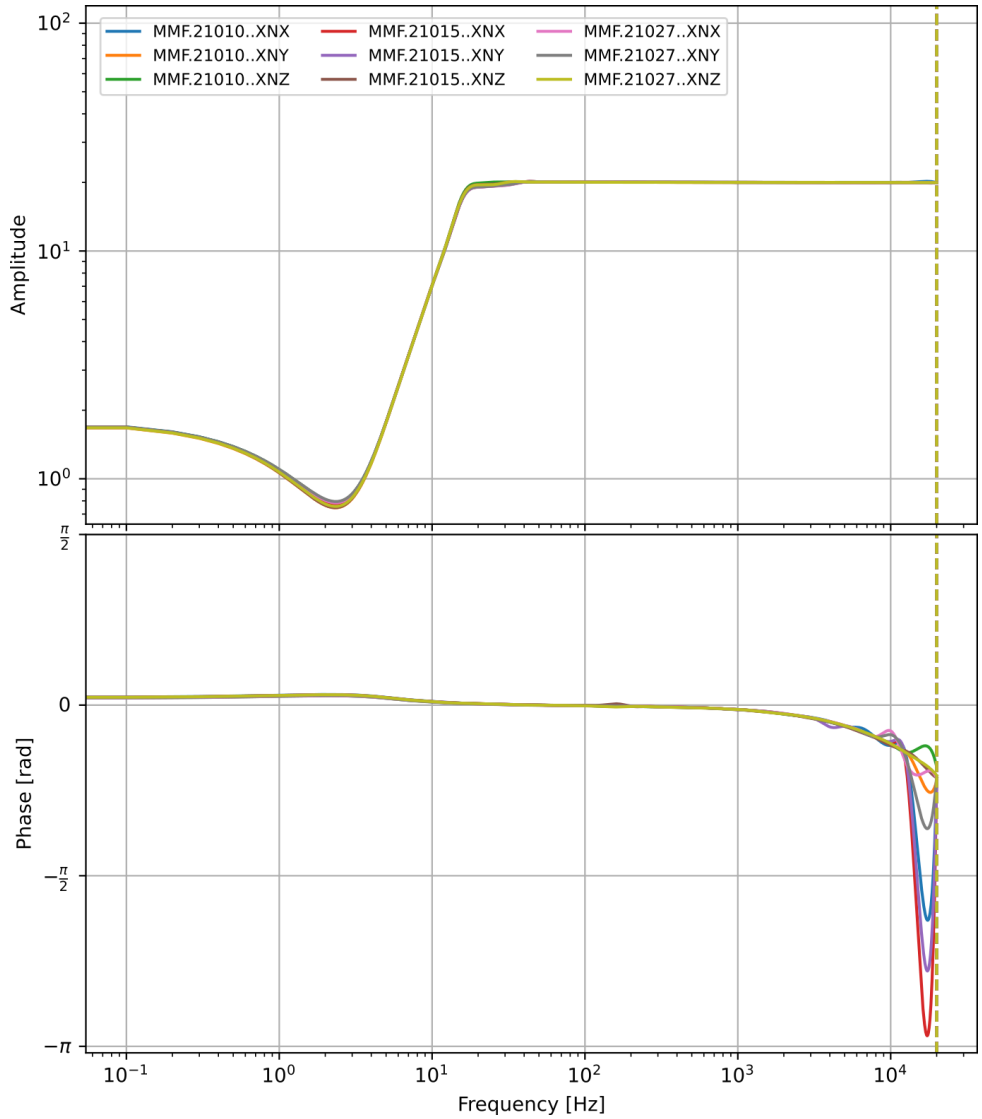

Figure 3: Acceleration amplitude (top) and phase (bottom) response for three of the 16 installed accelerometers. These results were obtained from a calibration certification process conducted by the sensor manufacturer MMF through a shake table test.

5 Results

When this report was written, results were only available through June 5, 2022. This was the date after which the realtime system stopped working and no further analysis of the continuous waveforms is possible until they are uploaded to servers at LBNL.

The final version of the catalog has been manually reviewed to both remove false detections and manually revise the phase arrival picks. This was necessary due to the low signal-to-noise ratio (SNR) of nearly all of the detected events, a consequence of the low sensitivity of the accelerometers (relative to those installed during the previous experiment). Following the revision of the events, we also relocated the seismicity with the NLLoc software (v6.0) using a homogenous velocity model ($V_p = 6900$ m/s, $V_s = 4100$ m/s, taken as an average from well logs).

Figure 4 shows the current final catalog from the start of the experiment until June 5, 2022. Figure **??** shows injection pressure and flow rate over the course of fracture creation and circulation testing. The seismicity detected on April 28 is actually the seismic manifestation of full waveform sonic logging of borehole TN and not seismicity in the usual sense.

The next obvious observation is that seismicity was not actually observed until May 6, which was one day after the start of injection into borehole TU. Injection had previously been into borehole TC from which a fracture had been driven all the way to the drift near the Site A alcove. It is safe to assume that the driving of a fracture many tens of meters from the point of injection was accompanied by seismicity, so the outstanding question is, “Why was seismicity detected once injection in TU exceeded 5000 psi at 5 L/min, and not during injection into TC?". There are three factors at play:

- The accelerometers installed in this testbed are one order of magnitude less sensitive than those installed in the previous testbed on the 4850 level.
- The period when seismicity began corresponds to the highest flow rates and injection pressures to that point in the experiment (5 L/min and 5000 psi)
- TU sits at the top of the injection well set (highest elevation), closer to sensors in AMU and DMU, but further from AML and DML.

While the decrease in sensor sensitivity certainly hampers our ability to detect smaller-magnitude seismicity (this is immediately obvious from the low SNR of the events we do detect), it doesn't explain the related inference that the seismicity associated with TU injection is therefore of a higher magnitude than the seismicity that, presumably, occurred during injection, and fracture creation, from TC. Partly, the larger magnitudes could be explained by the increase in pressure and flow rate, but we would still have expected to detect the seismicity associated with the fracture created from TC. It's possible that something about the rock mass in the upper portion of the testbed lends itself to larger

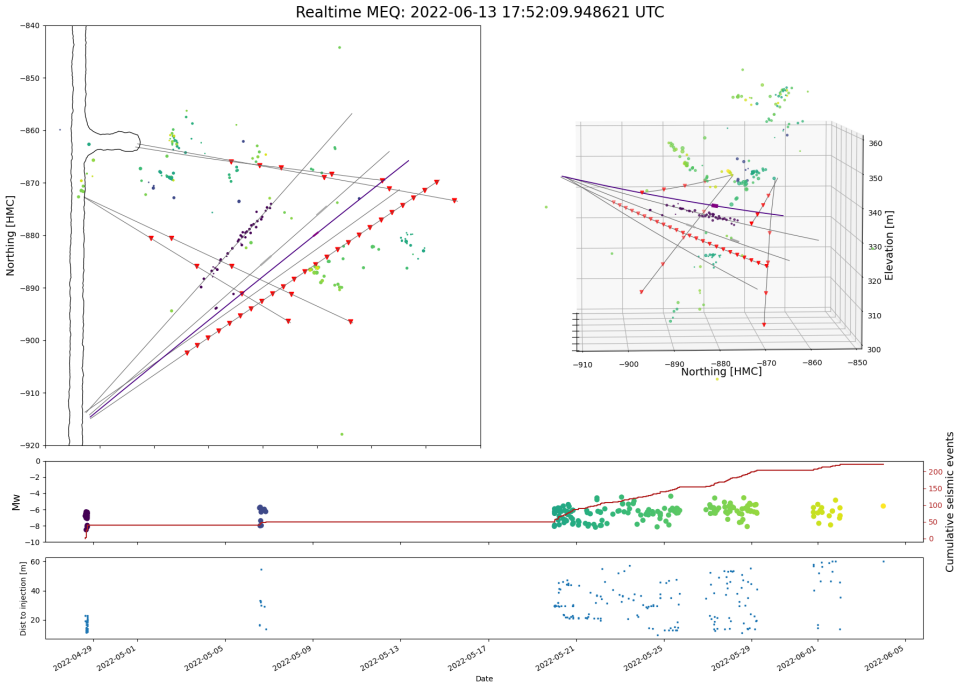

Figure 4: Acceleration amplitude (top) and phase (bottom) response for three of the 16 installed accelerometers. These results were obtained from a calibration certification process conducted by the sensor manufacturer MMF through a shake table test.

seismicity and/or more efficient propagation of seismic waves. The fact that we accurately detect and locate the FWS logging shots in TN, however, shows that we should have been able to detect seismicity along the fracture that passed directly through TN during injection into TC.

6 Appendices

6.1 VIBbox channel order

SEED id	Type of data
CB.TS02..XDH	Hydrophone
CB.TS04..XDH	Hydrophone
CB.TS06..XDH	Hydrophone
CB.TS08..XDH	Hydrophone
CB.TS10..XDH	Hydrophone
CB.TS12..XDH	Hydrophone
CB.TS14..XDH	Hydrophone
CB.TS16..XDH	Hydrophone
CB.TS18..XDH	Hydrophone
CB.TS20..XDH	Hydrophone
CB.TS22..XDH	Hydrophone
CB.TS24..XDH	Hydrophone
CB.AML1..XNX	Accelerometer
CB.AML1..XNY	Accelerometer
CB.AML1..XNZ	Accelerometer
CB.AML2..XNX	Accelerometer
CB.AML2..XNY	Accelerometer
CB.AML2..XNZ	Accelerometer
CB.AML3..XNX	Accelerometer
CB.AML3..XNY	Accelerometer
CB.AML3..XNZ	Accelerometer
CB.AML4..XNX	Accelerometer
CB.AML4..XNY	Accelerometer
CB.AML4..XNZ	Accelerometer
CB.AMU1..XNX	Accelerometer
CB.AMU1..XNY	Accelerometer
CB.AMU1..XNZ	Accelerometer
CB.AMU2..XNX	Accelerometer
CB.AMU2..XNY	Accelerometer
CB.AMU2..XNZ	Accelerometer
CB.AMU3..XNX	Accelerometer
CB.AMU3..XNY	Accelerometer
CB.AMU3..XNZ	Accelerometer
CB.AMU4..XNX	Accelerometer
CB.AMU4..XNY	Accelerometer
CB.AMU4..XNZ	Accelerometer
CB.DML1..XNX	Accelerometer
CB.DML1..XNY	Accelerometer

CB.DML1..XNZ	Accelerometer
CB.DML2..XNX	Accelerometer
CB.DML2..XNY	Accelerometer
CB.DML2..XNZ	Accelerometer
CB.DML3..XNX	Accelerometer
CB.DML3..XNY	Accelerometer
CB.DML3..XNZ	Accelerometer
CB.DML4..XNX	Accelerometer
CB.DML4..XNY	Accelerometer
CB.DML4..XNZ	Accelerometer
CB.DMU1..XNX	Accelerometer
CB.DMU1..XNY	Accelerometer
CB.DMU1..XNZ	Accelerometer
CB.DMU2..XNX	Accelerometer
CB.DMU2..XNY	Accelerometer
CB.DMU2..XNZ	Accelerometer
CB.DMU3..XNX	Accelerometer
CB.DMU3..XNY	Accelerometer
CB.DMU3..XNZ	Accelerometer
CB.DMU4..XNX	Accelerometer
CB.DMU4..XNY	Accelerometer
CB.DMU4..XNZ	Accelerometer
CB.CMon..	CASSM Monitor
CB.CTrig..	CASSM Trigger
CB.CEnc..	CASSM Source Encoder
CB.PPS..	Pulse per second time signal

Table 2: SEED names for each channel in the order stored in the VIBbox binary data files.

6.2 Seismic sensor locations

Station name	X [HMC ft]	Y [HMC ft]	Z [HMC ft]
TS01	4022.308614	-2960.480988	1105.456392
TS02	4028.730674	-2955.923056	1103.281251
TS03	4035.159656	-2951.361893	1101.133504
TS04	4041.658533	-2946.752842	1098.99255
TS05	4048.124287	-2942.168286	1096.891169
TS06	4054.603637	-2937.574515	1094.812869
TS07	4061.088634	-2932.977166	1092.76025
TS08	4067.579209	-2928.376291	1090.733326
TS09	4074.106998	-2923.750888	1088.719353
TS10	4080.624526	-2919.135762	1086.73056
TS11	4087.115853	-2914.542168	1084.771571
TS12	4093.604668	-2909.953319	1082.835051
TS13	4100.124222	-2905.347141	1080.916049
TS14	4106.699635	-2900.707122	1079.011584
TS15	4113.235412	-2896.100648	1077.149315
TS16	4119.779132	-2891.494103	1075.31533
TS17	4126.343224	-2886.87296	1073.501334
TS18	4132.87711	-2882.268382	1071.717443
TS19	4139.492447	-2877.601627	1069.933412
TS20	4146.045568	-2872.974048	1068.188082
TS21	4152.634164	-2868.32002	1066.45809
TS22	4159.187727	-2863.691775	1064.763952
TS23	4165.738106	-2859.066808	1063.097141
TS24	4173.156098	-2853.830083	1061.230863
AML1	4048.9701	-2841.082857	1076.228815
AML2	4079.264196	-2844.939494	1050.317648
AML3	4109.716412	-2848.916415	1024.377829
AML4	4140.207133	-2852.808518	998.5486472
AMU1	4066.106288	-2843.574918	1116.460595
AMU2	4105.277604	-2850.81498	1111.442245
AMU3	4144.562651	-2858.120697	1107.048016
AMU4	4183.847975	-2865.504628	1103.28804
DML1	4000.655148	-2889.068877	1092.552036
DML2	4028.111438	-2906.43786	1069.132752
DML3	4055.576022	-2923.61341	1045.66585
DML4	4083.337964	-2940.782028	1022.031092
DMU1	4013.037448	-2888.868988	1125.728398
DMU2	4049.216969	-2906.382033	1125.153255
DMU3	4085.221558	-2923.805786	1125.339731
DMU4	4121.212243	-2941.237009	1126.234317

Table 3: XYZ coordinates for each seismic sensor. The coordinates are in Homestake Mine Coordinates, which is a cartesian coordinate system used in the mine. Units are feet.

6.3 Python function to read raw, 32-bit VIBbox data to an Obspy Stream

```
import numpy as np

from scipy.stats import median_absolute_deviation
from obspy import Stream, Trace, UTCDateTime
from obspy.core.trace import Stats

import matplotlib.pyplot as plt


def vibbox_read(fname, seeds, debug=0):
    """
    Read function for raw VIBbox, 32-bit binary data files

    :param fname: Name of the file to read
    :param seeds: Iterable of the SEED ids in order stored on file
    :param debug: Debugging flag, basically to check time signal is
                                            being read
    :return:
    """
    network, stations, locations, channels = zip(*[s.split('.') for s in
                                            seeds])
    network = network[0]
    # Find channel PPS (pulse per second)
    try:
        clock_channel = np.where(np.array(stations) == 'PPS')[0][0]
    except IndexError:
        print('No PPS channel in file. Not reading')
        return
    # TODO Everything from here to file open should go in config?
    HEADER_SIZE=4
    HEADER_OFFSET=27
    DATA_OFFSET=148
    VOLTAGE_RANGE=10  # +/- Volts
    with open(fname, "rb") as f:
        f.seek(HEADER_OFFSET, os.SEEK_SET)
        # read header
        H = np.fromfile(f, dtype=np.uint32, count=HEADER_SIZE)
        BUFFER_SIZE=H[0]
        FREQUENCY=H[1]
        NUM_OF_BUFFERS=H[2]
        no_channels=H[3]
        # read data
        f.seek(DATA_OFFSET, os.SEEK_SET)
        A = np.fromfile(f, dtype=np.uint32,
                        count=BUFFER_SIZE * NUM_OF_BUFFERS)
        try:
            A = A.reshape(int(len(A) / no_channels), no_channels)
        except ValueError as e:
            print(e)
            # File was interrupted mid-write. Return empty stream
            return Stream()
```

```
    # Sanity check on number of channels provided in yaml
    if len(channels) != no_channels:
        print('Number of channels in config file not equal to number in
                                                data')
        return
    A = A / 2**32  # Norm to 32-bit
    A *= (2 * VOLTAGE_RANGE)
    A -= VOLTAGE_RANGE  # Demean
    path, fname = os.path.split(fname)
    try:
        # Use derivative of PPS signal to find pulse start
        dt = np.diff(A[:, clock_channel])
        # Use 70 * MAD threshold
        samp_to_first_full_second = np.where(
            dt > np.mean(dt) + 30 * median_absolute_deviation(dt))[0][0]
        # Condition where PPS not recorded properly
        if samp_to_first_full_second > 101000:
            print('Cannot read time signal')
            return
        # If we start during the time pulse, use end of pulse for timing
        if samp_to_first_full_second > 90000:
            print('Start of data is during time pulse. Using end of
                                                pulse.')
            # Negative dt
            samp_to_first_full_second = np.where(
                dt < np.mean(dt) - 30 *
                median_absolute_deviation(dt))[0][0] + 90000
        if debug > 0:
            fig, ax = plt.subplots()
            ax.plot(dt, color='r')
            ax.plot(A[:, clock_channel], color='k')
            ax.axhline(y=np.mean(dt) + 30 * median_absolute_deviation(dt
                                                ),
                       color='magenta', linestyle='--')
            ax.axvline(x=samp_to_first_full_second, color='magenta',
                       linestyle='--')
            fig.text(x=0.75, y=0.75, s=samp_to_first_full_second,
                     fontsize=14)
            plt.show()
        starttime = UTCDateTime(
            np.int(fname[5:9]), np.int(fname[9:11]), np.int(fname[11:13]
                                                ),
            np.int(fname[13:15]), np.int(fname[15:17]), np.int(fname[17:
                                                19]),
            np.int(1e6 * (1 - (np.float(samp_to_first_full_second) /
                               FREQUENCY))))
    except Exception as e:
        print(e)
        print('Cannot read exact time signal: ' + fname +
              '. Taking an approximate one instead')
        starttime = UTCDateTime(
            np.int(fname[5:9]), np.int(fname[9:11]), np.int(fname[11:13]
                                                ),
            np.int(fname[13:15]), np.int(fname[15:17]), np.int(fname[17:
                                                19]),
```

```
            np.int(1e2 * np.int(fname[19:23])))
    # arrange it in an obspy stream
    st = Stream()
    for i, sta in enumerate(stations):
        stats = Stats()
        # stats.sampling_rate = round(H[1], 1)
        stats.delta = 1. / H[1]
        stats.npts = A.shape[0]
        stats.network = network
        stats.station = sta
        stats.channel = channels[i]
        stats.location = locations[i]
        stats.starttime = starttime
        # Create new array to avoid non-contiguous warning in obspy.core
                                                .mseed
        st.traces.append(Trace(data=np.array(A[:, i]), header=stats))
    return st
```

6.4 Borehole design cross-sections

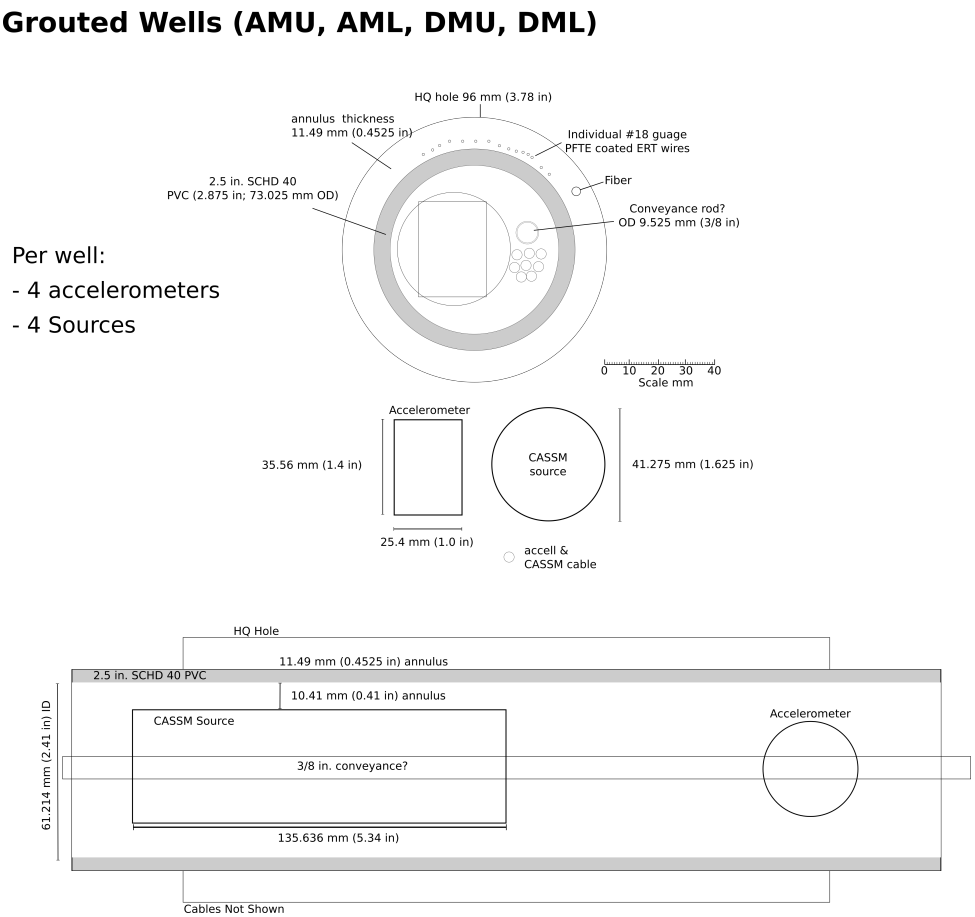

Figure 5: Scale cross-section of the grouted boreholes AMU, AML, DMU, DML showing all equipment installed in these boreholes.

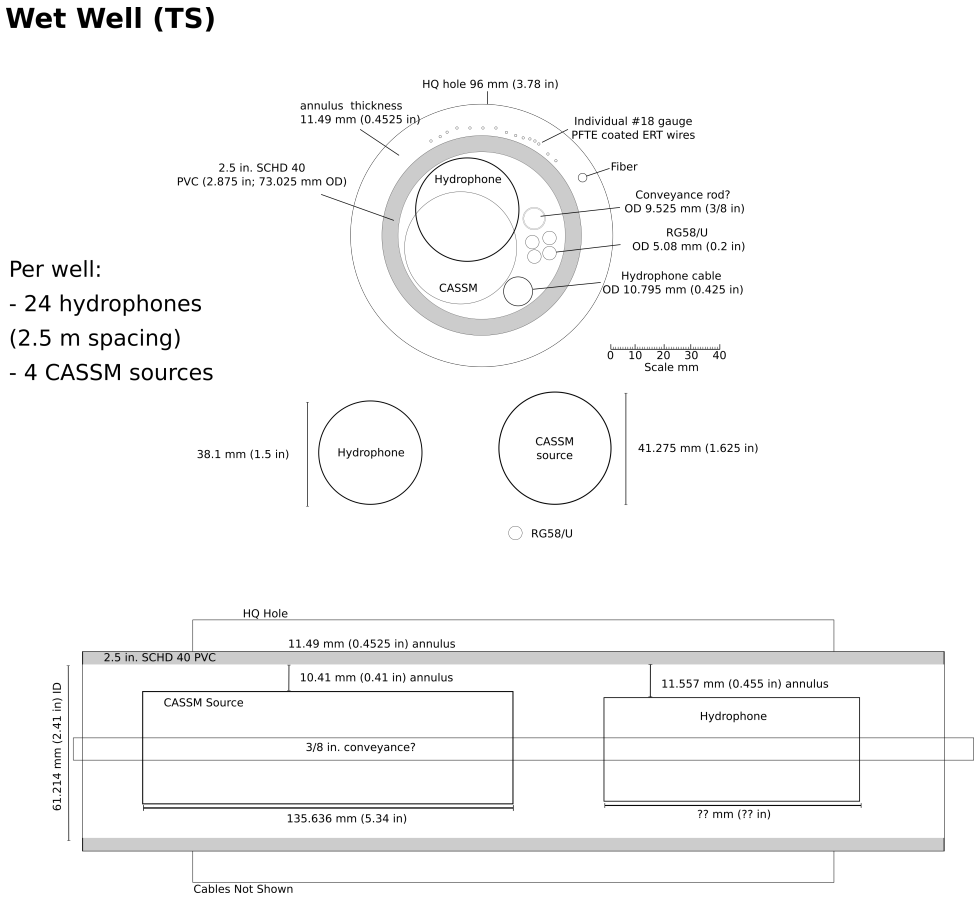

Figure 6: Scale cross-section of the non-grouted (i.e. wet) borehole, TS, showing all equipment installed.

6.5 Center punch calibration shot points

Shot pt name	X [HMC m]	Y [HMC m]	Z [HMC m]
S-1	3999.726	-2758.007	1126.956
S-2	3994.419	-2790.907	1126.421
S-3	3991.186	-2818.472	1125.364
S-4	3984.619	-2854.833	1126.722
S-5	3978.965	-2887.941	1125.982
S-6	3973.136	-2921.056	1126.629
S-7	3970.155	-2943.064	1126.278
S-8	3963.764	-2980.992	1127.543
S-9	3954.997	-3036.468	1126.018
S-10	3950.652	-3067.296	1126.359
S-11	3945.863	-3094.749	1125.745

Table 4: XYZ coordinates for each calibration shot point.

6.6 Center punch calibration shot times

Time of hammer (+/-0.5 sec UTC)	Shot point
3/8/2022 22:54:20	S-1
3/8/2022 22:55:30	S-2
3/8/2022 22:58:10	S-4
3/8/2022 22:59:20	S-5
3/8/2022 23:00:30	S-6
3/8/2022 23:01:30	S-7
3/8/2022 23:02:50	S-8
3/8/2022 23:05:30	S-10
3/8/2022 23:04:30	S-11
3/11/2022 19:00:00	S-1
3/11/2022 19:01:00	S-2
3/11/2022 19:02:20	S-4
3/11/2022 19:03:50	S-5
3/11/2022 19:04:50	S-6
3/11/2022 19:05:50	S-7
3/11/2022 19:06:50	S-8
3/11/2022 19:08:20	S-10
3/11/2022 19:09:20	S-11
3/11/2022 19:10:20	S-10
3/11/2022 19:11:30	S-8
3/11/2022 19:12:30	S-7
3/11/2022 19:13:20	S-6
3/11/2022 19:14:20	S-5
3/11/2022 19:15:20	S-4
3/11/2022 19:16:20	S-2
3/11/2022 19:17:20	S-1
3/11/2022 19:19:50	S-2
3/11/2022 19:26:00	S-4
3/11/2022 19:27:00	S-5
3/11/2022 19:28:00	S-6
3/11/2022 19:28:50	S-7
3/11/2022 19:29:40	S-8
3/11/2022 19:31:40	S-10
3/11/2022 19:32:30	S-11
3/11/2022 19:34:00	S-10
3/11/2022 19:35:10	S-8
3/11/2022 19:36:10	S-7
3/11/2022 19:37:00	S-6

3/11/2022 19:38:30	S-5
3/11/2022 19:39:30	S-4
3/11/2022 19:41:40	S-2
3/11/2022 19:42:30	S-1
4/13/2022 16:23:00 (Aprrox)	S-4
4/22/2022 19:26:00	S-1
4/22/2022 19:26:50	S-2
4/22/2022 19:27:40	S-3
4/22/2022 19:29:00	S-4
4/22/2022 19:30:00	S-5
4/22/2022 19:30:50	S-6
4/22/2022 19:32:00	S-8
4/22/2022 19:34:20	S-10
4/22/2022 19:35:10	S-11
4/22/2022 19:36:10	S-10
4/22/2022 19:37:40	S-6
4/22/2022 19:38:30	S-5
4/22/2022 19:39:20	S-4
4/22/2022 19:40:10	S-3
4/22/2022 19:41:00	S-2
4/22/2022 19:41:50	S-1

Table 5: Timing of the hammer shot preceding ten center punch shots at the specified shot point.

References

[1] Calum J. Chamberlain, Chet J. Hopp, Carolin M. Boese, Emily Warren-Smith, Derrick Chambers, Shanna X. Chu, Konstantinos Michailos, and John Townend. EQcorrscan: Repeating and Near-Repeating Earthquake Detection and Analysis in Python. *Seismological Research Letters*, 89(1):173–181, 12 2017.

[2] Thomas M. Daley, Ray D. Solbau, Jonathan B. Ajo-Franklin, and Sally M. Benson. Continuous active-source seismic monitoring of CO2 injection in a brine aquifer. *Geophysics*, 72(5):A57–A61, 07 2007.